Journal of Mechatronics Engineering

Evaluation of synchronizer geometric and tribological parameters and its influences to phases of synchronization through simulation in GT-Suite

ROMULO DO NASCIMENTO RODRIGUES[1,2], GABRIELA ACHTENOVÁ[1], LUKÁŠ KAZDA[1]

[1]Centre of Vehicles for Sustainable Mobility, Faculty of Mechanical, Czech Technical University, Praghe, Czech Republic
[2]Laboratory of Vibration - Labvib, Mechanical Engineering Department, Federal University of Ceará, Fortaleza, Brazil

<romulo.rodrigues@cvut.cz>, <gabriela.Achtenova@fs.cvut.cz>, <lukas.kazda@fs.cvut.cz>

DOI: 10.21439/jme.v8i1.119

Abstract. The transmission system is a vital component that significantly affects a vehicle's performance, power, and fuel efficiency. As vehicle technologies advance, demands on transmission systems continue to increase, with performance often evaluated through gear efficiency, noise levels, and the comfort of gear shifts. Among the key parameters for transmission system performance, synchronization time plays a crucial role. While previous studies have proposed mathematical and computational models of synchronization processes validated by experimental data, limited work has employed GT-Suite software. This article models a gear shift mechanism in GT-Suite to explore the synchronization process phases and analyze parameters influencing synchronization time. The study examines structural and tribological design parameters, evaluating their individual and collective impact on synchronization time. The results demonstrate the influence of varying parameters on the synchronization process, identifying critical phases where each parameter has the most significant effect. These findings provide valuable insights into optimizing synchronization mechanisms and reducing gear-shifting time. Future work may focus on expanding the parameter range and integrating experimental validation to enhance the model's applicability further.

Keywords: Gear shifting mechanism; Synchronization time; GT-Suite; Friction; Automotive gearbox.

(Received: December 10^{th}, 2024 / Accepted: January 21^{st}, 2025)

1 Introduction

Automotive industry is struggling to meet the future demands in order to reduce carbon dioxide emissions. In this regard different components of the vehicle (engine design, drivetrain etc.) are under consideration to update (IRFAN; BERBYUK; JOHANSSON, 2019). The gearbox, inclusive of its gear-shifting mechanism, plays a pivotal role in the drivetrain. The synchronizer, a component of the gear-shifting mechanism, is essential for ensuring swift, seamless, and energy-efficient transitions. This is imperative to align with the evolving technological advancements in the automotive industry. As an illustration of the necessity to enhance components in order to better align with increasing demands, can refer to the research conducted by Shiheng Sun and Huiting Shi (SUN; SHI, 2017). An automatic shift sys-

tem is designed for Taishan TG1804 tractor to make the gear shift easier and shorter. The test results show that the newly designed shifting mechanism has better reliability and a shorter shift time compared with the original shifting mechanism (SUN; SHI, 2017).

Gear shift quality is traditionally optimized in a vehicle on the road through the evaluation of the driver's perception. This classical human-feedback-based method faces different challenges, such as low reproducibility and high cost (HUANG; GUHMANN, 2018). The devised framework is composed of a dynamic model of the transmission system, an adaptive gear shift controller, an objective assessment of the gear shift quality, and a multi-objective optimization algorithm. The case study with an AMT synchronization system shows that this algorithm can effectively obtain the optimal shift trajectory, and the validation on the test bench proves that the optimized gear shift process has a high quality.

Nejad, in his research, states that reducing the transmission time will increase the efficiency of the transmission system and minimize the energy loss during the shifting process (NEJAD; CHIANDUSSI, 2017). In order to achieve the optimized design, the time estimation for synchronizing process is necessary. In this study, the multi-body dynamic model is proposed to predict the synchronization time (NEJAD; CHIANDUSSI, 2017). Two different synchronizer geometries were used as case studies, and experimental tests were conducted on a particular test rig machine. Different angular speeds, inertia, friction coefficient, and axial load were used for the two test cases, and the synchronization time was calculated.

Häggström and Nordlander (HÄGGSTRÖM; NORDLANDER, 2011; BEDMAR, 2013), developed a program in matlab for calculating heavy truck gearbox synchronization. It was made to support different shift scenarios and different types of gearboxes. It was also considered the values of drag that had been experimentally measured. Hoshino (BEDMAR, 2013; HOSHINO, 1999) devised a simulation to elucidate the synchronization mechanism within a heavy-duty truck transmission. The shifting of gears was dissected into six distinct events, and an upshift was simulated. This study specifically examines the effects of shifting speed and friction coefficients. The simulation, executed at three different shifting speeds, yielded disparate initial contact points for the gear spline chamfer, consequently influencing the processes of spline meshing. It's important to note that despite these impacts on the synchronization mesh between the sleeve and the clutch gear, neither the linkages nor the drivetrain were incorporated in the simulation (BEDMAR, 2013).

Liu and Tseng (BEDMAR, 2013; LIU; TSENG, 2007), developed a simulation model for a strutless double-cone synchronizer during the transition from the first to the second gear ratio. This paper categorizes the simulations into two scenarios: the synchronized module and the meshing module, contingent on the position of the sleeve. The rationale behind this division stems from the observation that previous simulation results, encompassing both displacement and relative rotational velocity, remained consistent until the engagement with the outer ring was completed, after which they exhibited variations. In the second scenario, the stochastic meshing process between the sleeve and the clutch gear was further subdivided into four distinct situations. This segregation was necessitated by the diverse movements contingent on different mesh angles between the sleeve and the clutch gear(BEDMAR, 2013). Specific mesh angles prompted both forward and backward movements of the sleeve, whereas at certain mesh angles, the sleeve exclusively advanced. It is noteworthy that the delineation between these sections would be altered with any modification to the simulation conditions.

Irfan, Berbyuk e Johansson (2015b) state that robust and efficient synchronizers are keys elements to ensure good gear shift in heavy vehicles, and,in order to improve existing as well as develop new synchronizers, efficient simulation tools are needed. In his various publications (IRFAN; BERBYUK; JOHANSSON, 2019; IRFAN; BERBYUK; JOHANSSON, 2015b; IRFAN; BERBYUK; JOHANSSON, 2015a), studies were carried out with a mechanical system with 5 degrees of freedom modeling a generic synchronizer consisting of engaging sleeve, synchronizer ring, and gearwheel are considered. Due to the design of the different components and their interactions the synchronizing process is described in terms of different steps or phases, presynchronization, main synchronization, blocker transition and engagement. Using Constrained Lagrangian Formalism (CLF), and MATLAB and GT Suite software, a mathematical model of a generic synchronizer is developed and represented by the system of differential-algebraic equations. Through these models, it was possible to simulate the mechanisms and analyze the behavior of certain parameters regarding failure and synchronization time in heavy vehicles.

Several researchers, such as Huang (HUANG et al.,

2015), Li (LI et al., 2017), Zainuri (ZAINURI et al., 2017), and Qi (QI et al., 2017), have developed simulation models to better understand the synchronization mechanism and the factors that influence it, including those related to failure or performance. In line with these efforts, this article aims to investigate the parameters that influence the reduction of gear shifting time through simulation. The gear shift mechanism (Figure 1) is modeled using GT-Suite software, chosen due to the lack of literature exploring its use to analyze the phases of the synchronization process and the parameters that influence these phases. The primary objective of the model is to describe and evaluate the different phases involved in the synchronization mechanism process, enabling a detailed understanding of how these phases interact. The model will allow for the identification of key parameters that influence synchronization time, including both structural and tribological design factors. By varying these parameters, the study aims to assess their actual impact on synchronization time and provide insights into optimizing the synchronization process.

The reduction of synchronization time in the gear shifting mechanism is highly relevant, especially in the context of current demands in the automotive industry. With the growing focus on fuel efficiency and the reduction of CO_2 emissions, optimizing the gear shifting process can significantly contribute to a smoother and more efficient driving experience. Faster and more precise gear shifts not only improve fuel economy but also reduce environmental impact, both of which are crucial for meeting the industry's increasingly stringent sustainability and performance standards. Therefore, this research aims to provide a deeper understanding of the parameters that influence synchronization time, offering solutions that can result in more efficient transmission systems aligned with the environmental and performance goals of modern vehicles.

This work makes a significant contribution to the literature by addressing the reduction of synchronization time in gear-shifting mechanisms using GT-Suite software, a tool rarely explored in this specific context. The proposed approach details the phases of the synchronization mechanism, enabling an in-depth analysis of the structural and tribological parameters that influence synchronization time. Furthermore, the article presents an innovative methodology that can be applied to different transmission configurations, with the potential to improve the efficiency and performance of automotive transmission systems. To facilitate the reader's understanding, the remainder of the article is organized as follows: Section 2 discusses the phases of gear synchronization, Section 3 presents the experimental measurements conducted, Section 4 details the modeling of the gear-shifting mechanism, and Section 5 presents the results and discussion. Finally, Section 6 concludes the study, highlighting its main contributions and suggesting directions for future work.

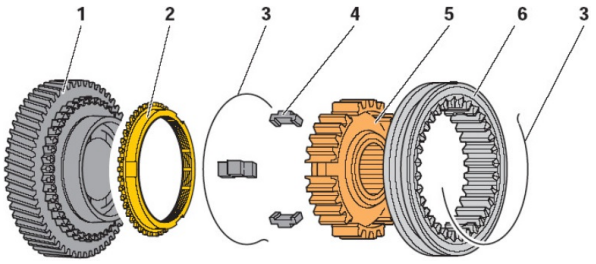

Figure 1: Borg-Warner(VW) single cone synchro clutch (ZEMAN, 2019). 1 - gear wheel; 2 -synchronizer ring; 3 - ring spring; 4 - locking element (strut); 5 - synchronizer hub (body) and 6 - sliding sleeve.

2 Gear synchronization phases

Depending on sources and specific synchronizer designs the number of phases varies, but the working principle is the same (BEDMAR, 2013). The synchronization process is going to be described using the parameters: F (N) – gearshift force, $\Delta\omega$ (rad/s) – speed difference between gear wheel and synchronizer hub,T_f (Nm) – friction torque between the synchronizer ring and friction cone and T_i (Nm) – inertia torque of the input shaft, gears and clutch secondary mass. The synchronization process involves five steps (ZEMAN, 2019), commencing with the sliding sleeve positioned neutrally (at the center) and culminating in a complete gear engagement, as illustrated in the Figure 2 .

Phase 1 Asynchronizing: Prior to initiating the gearshift process, the locking elements securely maintain the sliding sleeve in the central position. The application of the gearshift force induces axial movement in the sliding sleeve, propelling the synchronizer ring towards the friction cone gear wheel. The resulting speed difference between the gear wheel and the synchronizer ring initiates the rotation of the synchronizer ring.

Phase 2 Synchronizing (locking): This constitutes the primary stage of speed synchronization. The sliding sleeve undergoes additional displacement, causing the internal splines (teeth) of the sliding sleeve to come into the contact with the teeth of the synchronizer ring (blocking teeth). During this phase, the friction torque

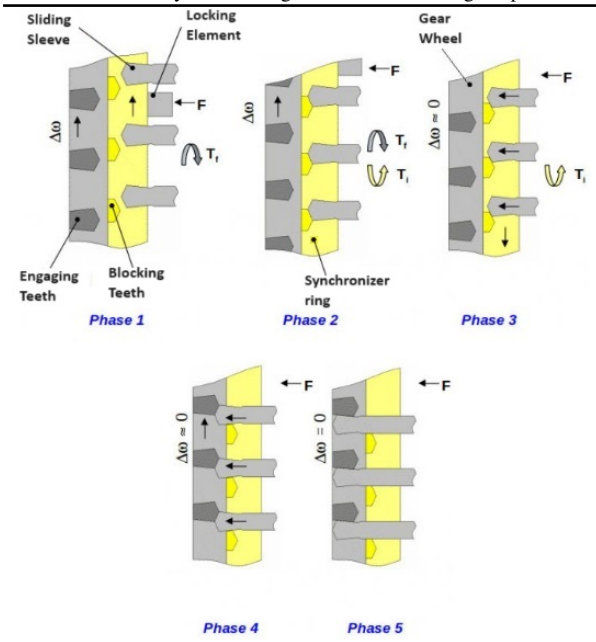

Figure 2: Gearshift synchronization process (adapted) (ZEMAN, 2019).

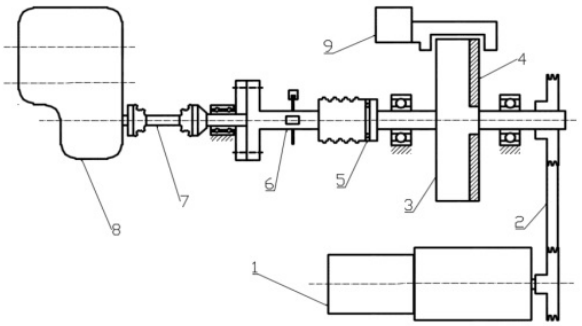

Figure 3: Test bench schematic.(ZEMAN, 2019) 1-Electric motor with external ventilation; 2-Belt transmission; 3-Flywheel; 4-Additional disc; 5-Flexible safety coupling; 6-Tensometer shaft for torque detection; 7-Articulated shaft; 8-Gearbox with integrated distribution box; 9 -emergency brake.

comes into play, opposing the inertia torque, and consequently, the speed difference begins to decrease.

Phase 3 Unlocking (turn back synchronizer ring): The gearshift force is maintained on the synchronizer ring by the locking elements and the sliding sleeve. Once speed synchronization is attained, the friction force diminishes to zero, and the synchronizer ring is turned back slightly.

Phase 4 Meshing (turn synchronizer hub): The sliding sleeve passes through the teeth of the synchronizer ring and comes into contact with the engaging teeth of the gear wheel.

Phase 5 Engaging (gear lock): The sliding sleeve has completely moved into the engaging teeth of the gear wheel. Back tapers at the teeth of the sliding sleeve and the gear wheel engaging teeth avoid decoupling under load.

3 Experimental measurements

The test stand located in the CTU laboratories was developed mainly by Ing. Jiří Pakosta, PhD (ZEMAN, 2019). Its purpose is to simulate operating conditions and, mainly, to test the durability of shaft reducers and their components (Figure 3). A flywheel is connected to the output of the gearbox under test to simulate the movement of the vehicle and its inertial masses. The flywheel is driven by an asynchronous electric motor with a power of 18.5 kW and its speed is controlled using a PID controller. The flywheel parameters are: diameter 620 mm with moment of inertia 14 kgm^2 and weight 300 kg. The driving torque from the flywheel to the gearbox is subsequently directed through the hollow shaft, which is glued with strain gauges and serves to measure the torque.

A pneumatic shifting robot is used to shift the gearbox (Figure 4). Utilizing six pneumatic cylinders, the system simulates the gear lever mechanism and controls the transmission's gear-shifting mechanism through two cables. The air pressure entering the cylinders is regulated by a proportional reducing valve, allowing for the adjustment of shift force levels for each individual shift. The NI LabVIEW environment with programmed control software is used for control and measurement data processing. The primary drawback of this experimental setup for the measurements employed in this research lies in its emphasis on long-term durability tests rather than single-shift dynamic tests (ZEMAN, 2019).

The measurement took place under stable conditions, and the measured individual displacements should not be influenced by external conditions. Due to the operating viscosity of the oil, whose temperature dependence significantly affects the smoothness and progress of the shift, it is recommended to maintain the oil filling temperature at least above 40^{o}C, but ideally above 45^{o}C. During the test, for this reason, the oil filling temperature was maintained in the range of 47 -

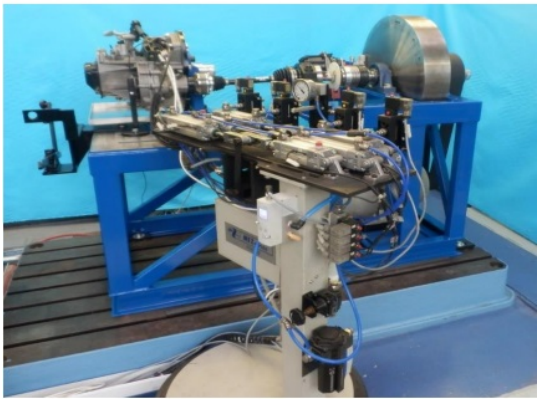

Figure 4: Experimental bench without covering the main parts (ZEMAN, 2019).

49^{o}C (ZEMAN, 2019). The maximum possible displacement force generated by the pistons is then limited by means of reducing valves to 180 - 200 N. Tests were carried out on a simple synchronization model with a Borg-Warner mechanism with a synchronization ring and retention lock similar to that in Figure 1. Controlling the shift levers using pneumatic pistons has a different stroke and force response than a real driver. This difference is due, in principle, to the great recoil damping that the system has. After switching on, the robot is configured to maintain additional force to stabilize the system.

The total synchronization time measured in the experimental test was 0.3 s (Figure 5). The time remained similar for shifts between 3^{rd} and 4^{th} (Figure 5 a) gear and between 4^{th} and 3^{rd} gear (Figure 5 b). Despite possible experimental deficiencies due to the fact that the test bench is not configured for this type of test, it was considered that the measured data are adequate to discover or specify the data that will be inserted into the GT-Suite model.

4 Modeling of a gear shifting mechanism

The gear shifting mechanism is modeled in GT-Suite with three rigid bodies: sleeve, ring, and gear, as shown in Figure 6. The gear is considered a master which rotates with constant speed during the gear-shifting process. The sleeve and the ring are connected by a detent connection, rotational contact connection, and blocking teeth. The blocking teeth represent the teeth that connect the sleeve to the synchronizer ring. The sleeve and the gear have engaging teeth. The engaging teeth represent the teeth that connect the sleeve to the gear wheel. The

Parameter name	Notation	Value
Ball Radius Detent (mm)	R_D	2
Grove Angle Detent (^{o})	β_D	30
Detent Coefficient of Friction	μ_D	0.2
Groove Height Detent (mm)	H_D	1
Conical Surface Offset (mm)	O_D	6
Engaging Teeth Angle Left (^{o})	β_{E_L}	45
Engaging Teeth Angle Right (^{o})	β_{E_R}	45
Blocking Teeth Angle Left (^{o})	β_{B_L}	45
Blocking Teeth Angle Right (^{o})	β_{B_R}	45
Cone Angle (^{o})	β_C	5
Cone Coefficient of Friction	μ_C	0.2
Blocking Teeth Friction Coefficient	μ_B	0.2
Engaging Teeth Friction Coefficient	μ_E	0.2
Cone Maximum Radius (mm)	$R_{C_{Max}}$	45
Cone Minimum Radius (mm)	$R_{C_{Min}}$	40
Undercut Angle Engaging Teeth (^{o})	α_B	5
Undercut Angle Blocking Teeth (^{o})	α_E	5
Blocking Teeth Radius (mm)	R_B	50
Engaging Teeth Radius (mm)	R_E	50
Number of Teeth Blocking	N_B	50
Number of Teeth Engaging	N_E	50
Lash Blocking Teeth (mm)	L_B	0.2
Lash Engaging Teeth (mm)	L_E	0.2
Ring Mass (g)	m_R	500
Gear Mass (g)	m_G	600
Sleeve Mass (g)	m_S	900
Ring Moment of Inertia (kgm^2)	I_R	0.04
Gear Moment of Inertia (kgm^2)	I_G	0.07
Sleeve Moment of Inertia (kgm^2)	I_S	0.07
Input Gear Rotational Speed (rpm)	ω	1000
Shift Force (N)	F_{Shf}	400

Table 1: Values of the structural design parameters of the generic synchronizers.

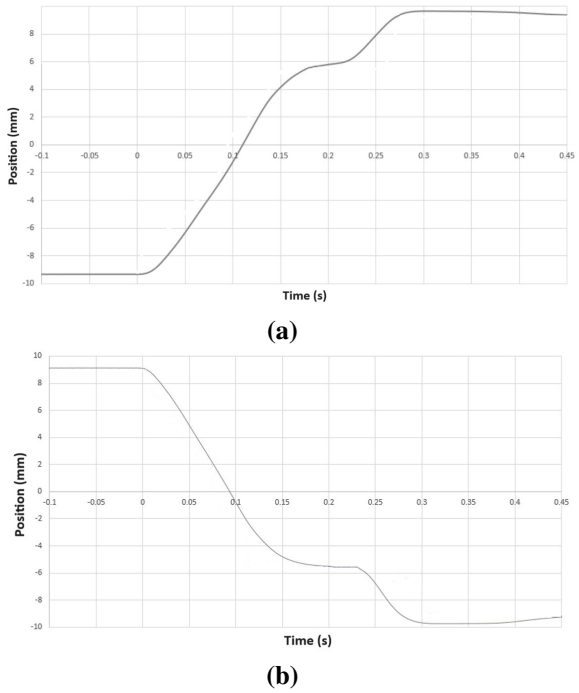

Figure 5: Position progress when shifting a) between 3^{rd} and 4^{th} gear b)between 4th and 3rd gear.

ring and the gear are connected by frictional cones. The gear shifting mechanism was simulated with the number of blocking and the engaging teeth set to 40, as per the real model. When the shift force is applied, the sleeve moves axially. The GT-Suite model is simulated, and the results are plotted in Figure 10. Values of the structural design parameters in GT-Suite are shown in Table 1. Some of the configurations of the main components used in the simulation can be seen in Figures 7, 8 and 9. Figure 7 presents a schematic representation of the retention latch utilized in the GT-Suite environment. In contrast, the simulated synchronizer (Figure 1) employs an expansion ring—a wire with a circular cross-section twisted into a circular shape, driven by retaining stones positioned at 120° intervals. Despite their differences, the functions are so similar that simply recalculating certain parameters is sufficient. The Groove Height (H_D), clearance G, and Grove Angle (β_D) are the same as the modeled gearbox lock. The radius of the ball, R_D, is selected based on the circularity of the latch stone's edges.

Analyzing the simulation results reveals the presence of all five synchronization phases. In the neutral position, the sleeve is centered through the use of the locking body and spring, eliminating the risk of spontaneous movement. When an axial force is applied, it is first necessary to overcome the locking force. During the movement of the sleeve Figure 7a, the locking spring of the centering mechanism also moves, pressing the shielding ring with its front surface and consequently the beginning of axial force begins to occur on the friction cone (Phase 1). In the sequence (Phase 2), the sleeve undergoes additional displacement, causing its internal splines (teeth) to slide and begin to engage the teeth of the synchronizer ring (Blocking Teeth)(Figure 7b). During this phase, the friction torque comes into play, opposing the inertia torque and, consequently, the speed difference begins to decrease. In the Phase 3,the gearshift force is maintained on the synchronizer ring by the locking elements and the sliding sleeve. Once speed synchronization is attained, the friction force diminishes to zero, and the synchronizer ring is turned back slightlyc(Figure 7b). The sleeve passes through the teeth of the Blocking Teeth (Phase 4) and comes into contact with the locking toothing (Engaging Teeth) (Figure 7c). In the Phase 5,the sleeve has completely moved into the Engaging Teeth of the gear wheel(Figure 7c). The total synchronization time in the simulation model was 0.29s, closely matching the experimental time of 0.3s.

With the GT Suite model adjusted and functional, enabling the identification of synchronization phases, the subsequent step involves varying specific parameters to assess their impact on synchronization time. The GT-Suite model was simulated by varying values of one of the parameters in a reasonable bounds while rest of this parameters have constant values. In this way, the influence of these parameters is identified, one by one, on the synchronization time. Geometric parameters of some key components of a basic synchronizer, along with the primary tribological parameter influencing synchronization time, in other words, the coefficient of friction between the components, were chosen for analysis. The parameters chosen for evaluation are listed in Table 2.

5 Results and discussion

The first parameter analyzed was the grove angle of detent (Figure 11). The variation grove angle of detent demonstrated an influence on the axial force of the detent, where with the increase in angle there was a small increase in the axial force. This variation in force has its influence, as shown in Figure 11, only at the conclusion

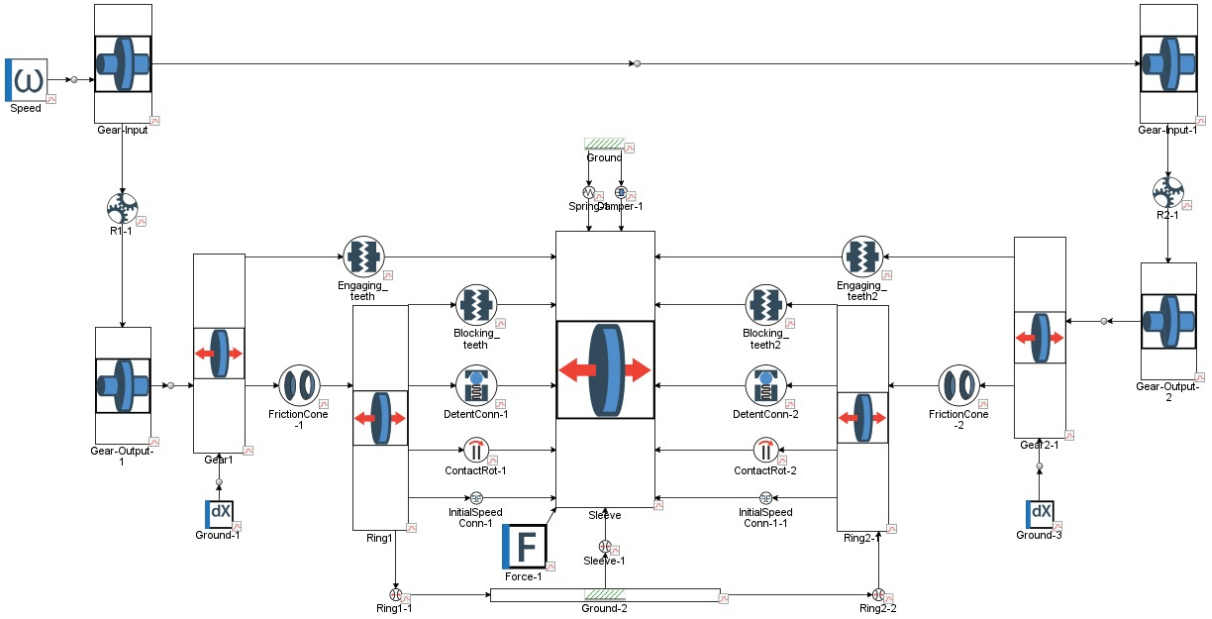

Figure 6: GT-Suite model of the generic synchronizer.

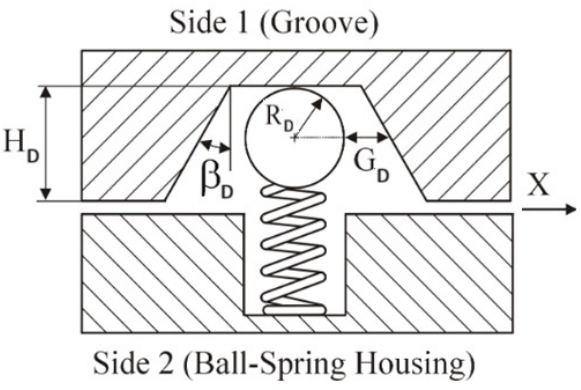

Figure 7: Detent Configuration.

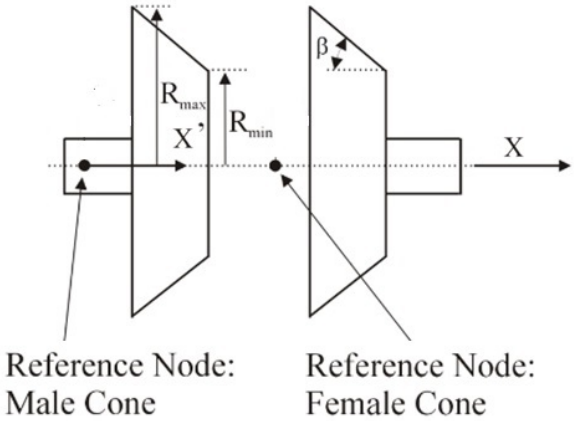

Figure 8: Cone Configuration.

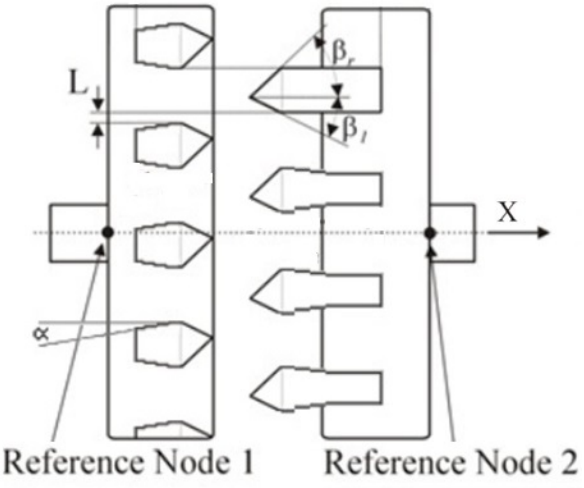

Figure 9: Blocking and Engaging Teeth Configuration.

Parameter name	Values
Grove Angle Detent (^{o})	[30 - 50]
Detent Coefficient of Friction	[0.15 - 0.35]
Groove Height Detent (mm)	[1 - 5]
Engaging Teeth Angle Left (^{o})	[20 - 45]
Engaging Teeth Angle Right (^{o})	[45 - 65]
Blocking Teeth Angle Left (^{o})	[20 - 45]
Blocking Teeth Angle Right (^{o})	[45 - 65]
Cone Angle (^{o})	[5 - 9]
Cone Coefficient of Friction	[0.15 - 0.35]
Blocking Teeth Friction Coefficient	[0.15 - 0.35]
Engaging Teeth Friction Coefficient	[0.15 - 0.35]
Cone Maximum Radius (mm)	[45 - 65]
Cone Minimum Radius (mm)	[20 - 40]
Lash Blocking Teeth (mm)	[0.1 - 0.5]
Lash Engaging Teeth (mm)	[0.1 - 0.5]

Table 2: Input parameter range values for analysis.

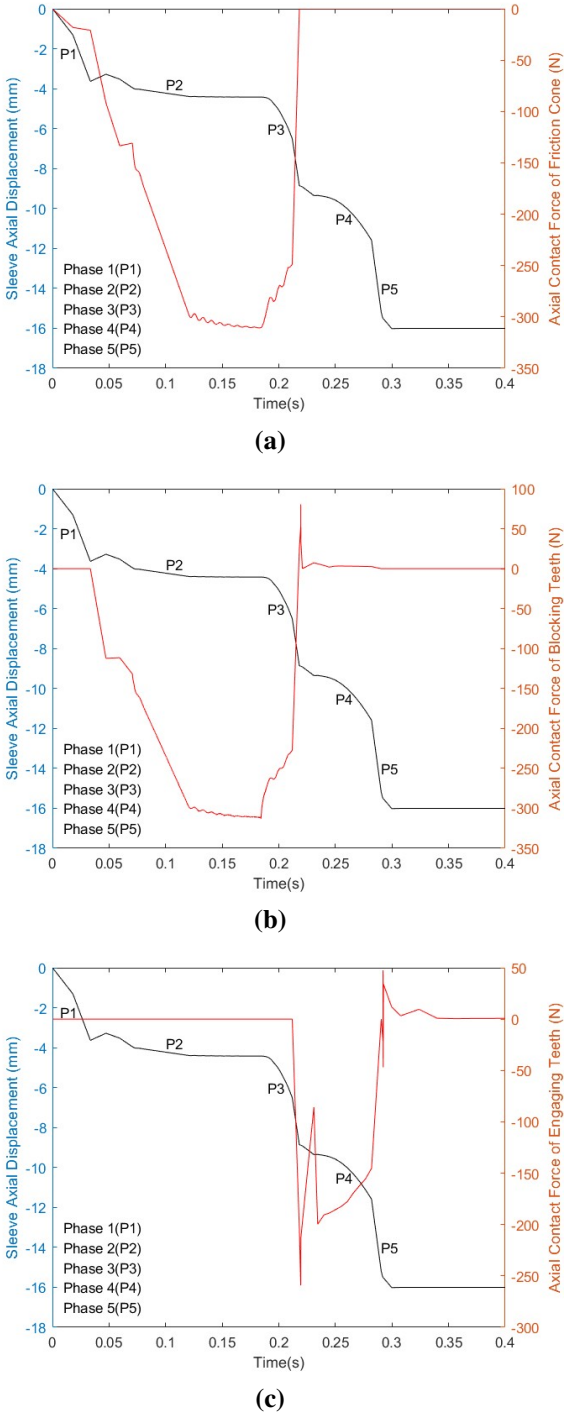

Figure 10: Synchronization performance of the gear shifting mechanism model in GT-Suite; (a) Sleeve Axial Displacement and Axial Contact Force of Friction Cone; (b) Sleeve Axial Displacement and Axial Contact Force of Blocking Teeth; (c) Sleeve Axial Displacement and Axial Contact Force of Engaging Teeth.

of phase 5, where there is a small increase in its time. Its impact on the synchronization time is not highly significant, resulting in an increase of mere fractions of a second, with the synchronization time remaining around 0.29s.

The variation in the friction coefficient of the detent yielded considerably more pronounced results in terms of its impact on synchronization time compared to the two previous parameters (Figure 12). The simulation results showed that increasing the friction coefficient produces a significant increase in the axial force acting on the detent. The increase in axial force produces greater resistance to the axial displacement of the synchronizer sleeve. This effect has an effect on all 5 synchronization phases, where all phases have their start and finish times increased, which consequently produces an increase in the final synchronization time. The results showed a time of 0.29s for the lowest coefficient of friction and 0.30s for the highest coefficient. The last parameter evaluated of the detent was the groove height (Figure 13). The model results indicate that increasing the value of the parameter leads to a notable increase in the vertical force exerted on the detent. The detent has a ring spring inside that is responsible for keeping the synchronizer sleeve motionless and centered when there is no force acting on the system (VIJAY et al., 2012) (Figure 1). The increase in the vertical force acting on the detent due to the increase in groove height provides faster deformation of the ring spring, which consequently reduces the resistance to axial displacement of the synchronizer sleeve. The variation of this parameter demonstrates a direct influence on phases 3, 4 and 5, which favors the reduction of the start and completion time of these phases. The final synchronization time for the highest parameter value was 0.27s and for the lowest value 0.29s.

The second component to be analyzed was the friction cone. Its purpose is to generate a friction torque that counteracts the inertia torque, thereby reducing the speed difference to prepare the components for coupling (STOCKINGER; SCHNEIDER; PFLAUM, 2020). The parameters evaluated were the friction coefficient, maximum and minimum radius, and cone angle.evidence of correct function of the model. The aim, in addition to understanding the influence of these parameters on the synchronization phases, was to evidence the correct functioning of the model. The first parameter to be analyzed in this component was its angle (Figure 14). The results obtained by model simulation indicate that increasing the cone angle causes a reduction

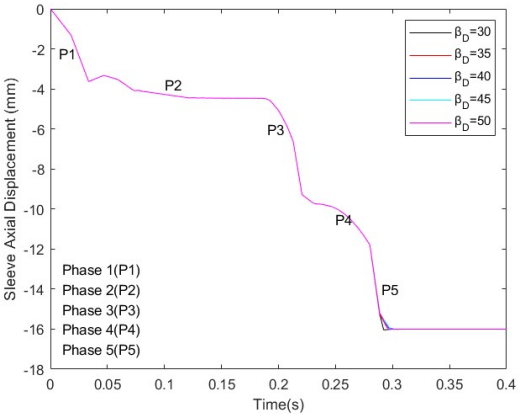

Figure 11: Variation of Grove Angle Detent in degrees.

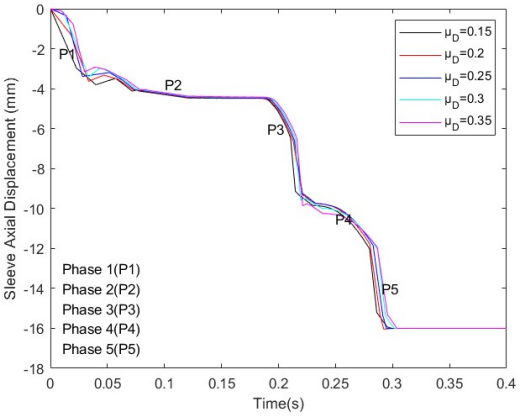

Figure 12: Variation of Detent Coefficient of Friction.

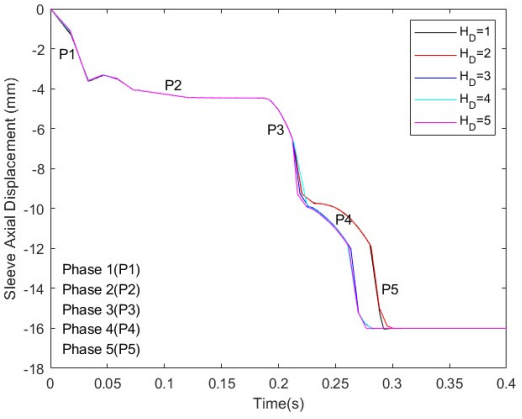

Figure 13: Variation of Groove Height Detent in mm.

in friction torque. This reduction in torque causes an increase in the time in which the cone will reduce rotation speed for synchronization to occur. The variation of this parameter has an influence on phases 2, 3, 4 and 5 and their start and completion times. The wedging condition of the sliding cones is not incorporated into this model. However, in practical applications, the wedging condition must be fulfilled; otherwise, the cones may become "welded"(self-locked) to each other during sliding.(IRFAN; BERBYUK; JOHANSSON, 2018) The maximum synchronization time obtained was 0.37 s for an angle of 9^o and a minimum of 0.29 s for an angle of 5^o.

The friction coefficient of the cone was also analyzed, and, as anticipated, it exerted a notable influence on the synchronization time (Figure 15). The increase in the friction coefficient generated an increase in the friction torque. As a result, the speed reduction time decreased, causing a reduction in the final synchronization time. This parameter directly and significantly influences phase 2 in its completion time. The final synchronization time for the highest parameter value was 0.24 s, and for the lowest value 0.29 s.

The increase in the maximum and minimum radius of the cone also showed to have their respective influence on the synchronization time (Figures 16 and 17). An elevation in both parameters resulted in an increased friction torque, consequently reducing the time required for rotational speed reduction. These parameters directly and significantly influence phase 2 in its completion time. It is crucial to note that when one of the radii was varied, the other remained constant. However, as noted by Irfan (IRFAN; BERBYUK; JOHANSSON, 2018), the factor that provides a greater increase in friction torque and consequently a reduction in synchronization time is the increase in the average radius of the cone. The final synchronization time for the highest value of the maximum radius was 0.27 s, and for the lowest value 0.29 s. For the minimum radius, the highest value resulted in 0.29 s and the lowest value 0.33 s.

In Figure 19, the results obtained by the model are illustrated for the variation of the tooth right angle of blocking teeth. The incremental change in the angle resulted in a minor adjustment to the required axial displacement for the synchronizer sleeve to initiate each phase affected. The parameter demonstrates influence on phases 2, 3, 4 and 5. While this parameter did impact certain phases, the overall increase in the final synchronization time was not particularly significant. There was a small decrease in time with the increase in an-

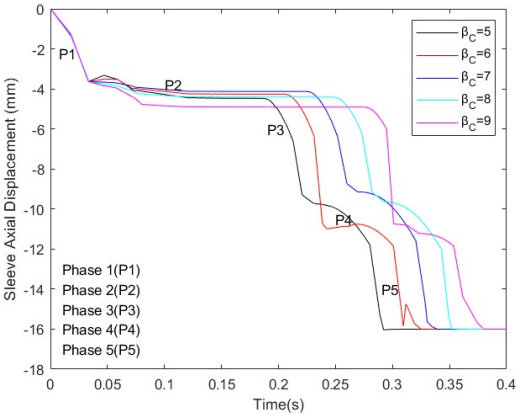

Figure 14: Variation of Cone Angle in degrees.

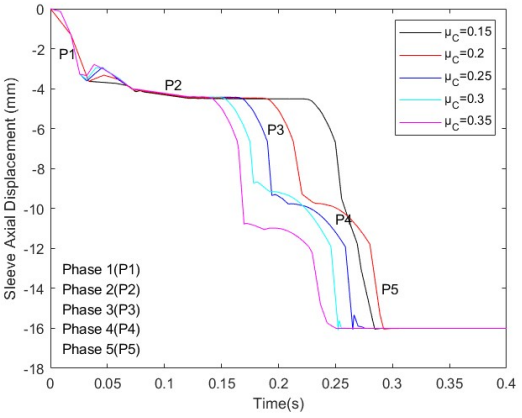

Figure 15: Variation of Cone Coefficient of Friction .

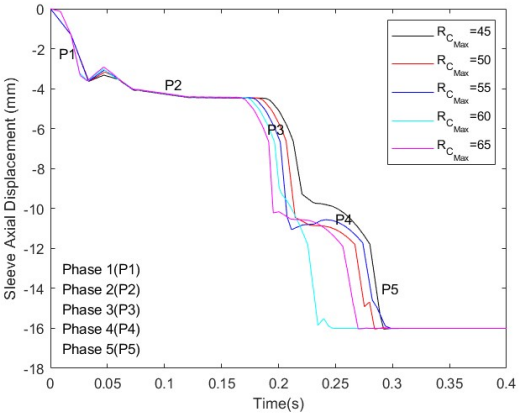

Figure 16: Variation of Cone Maximum Radius in mm.

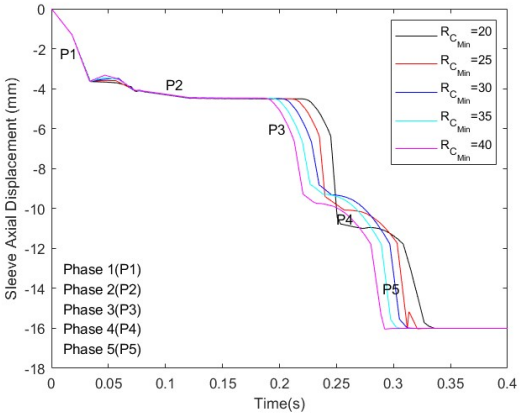

Figure 17: Variation of Cone Minimum Radius in mm.

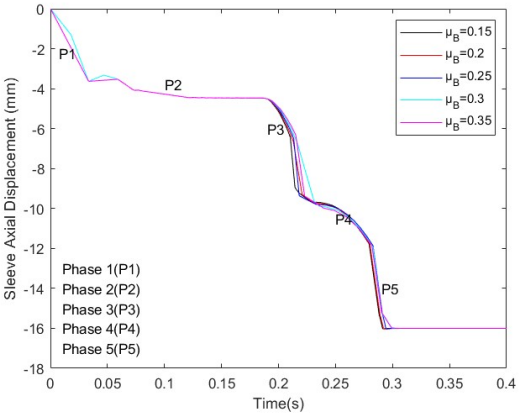

Figure 18: Variation of Blocking Teeth Friction Coefficient.

gle, where for the angle of 45^o, the time recorded was 0.29 s, whereas for the angle of 60^o, the time measured was 0.28 s. A similar behavior occurs when the parameter tooth left angle has been varied (Figure 20). The incremental change in the angle resulted in a minor adjustment to the required axial displacement for the synchronizer sleeve to initiate the phases 2, 3, 4 and 5. The displacement changes are greater, and therefore, generate a more significant variation in the final time. For this parameter, there was an increase in time with the increment in angle, where for the angle of 25^o, the time recorded was 0.27 s, whereas for the angle of 40^o, the time measured was 0.30 s.

The next component to be analyzed was the blocking teeth (synchronizer ring). The first parameter evaluated for this component was the friction coefficient, which demonstrated results as expected (Figure 18). The rise in the friction coefficient resulted in increased resistance to displacement, particularly noticeable during phase 3. This alteration led to shifts in both the initiation and completion times of this phase. While this did cause a slight uptick in synchronization time, the increase wasn't substantial. This is attributed to the system overcoming the initial resistance to displacement in phase 3, allowing the subsequent phases 4 and 5 to proceed without significant disruption. The final synchronization time for the highest parameter value was 0.30 s and for the lowest value 0.29 s.

The last parameter evaluated for the blocking teeth was lash or free-play between teeth (Figure 21). Varying this parameter also changed the displacement of the synchronizer sleeve, affecting phases 2 to 5. Although it generated a change in the phases, especially

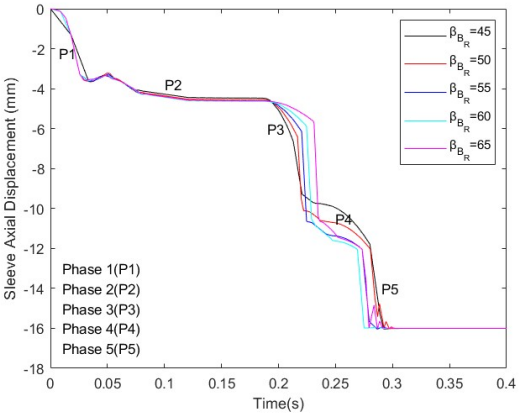

Figure 19: Variation of tooth right angle of Blocking Teeth in degrees.

in phase 4, the change in the final time was not significant, being in the thousands of seconds. For all parameter values, the final synchronization time is around 0.29 s.

The last component to be analyzed was the engaging teeth (gear wheel). The first parameter evaluated for this component was the friction coefficient, which demonstrated results as expected (Figure 22). Similar to blocking teeth, the rise in the friction coefficient resulted in increased resistance to displacement, particularly noticeable during phase 4 and 5. This alteration led to shifts in both the initiation and completion times of these phases. In contrast to the situation observed in the blocking ring, the friction coefficient for this component exhibited a more pronounced and gradual increase in the time. The final synchronization time for the

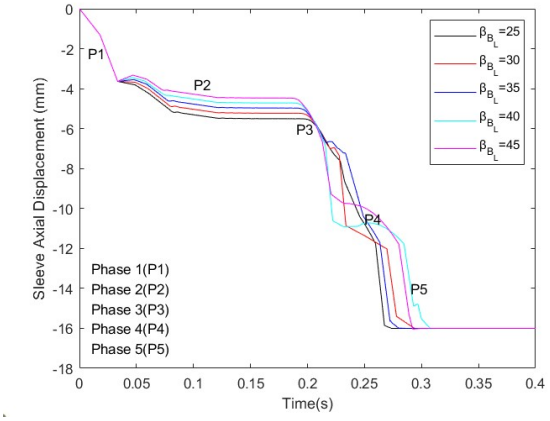

Figure 20: Variation of tooth left angle of Blocking Teeth in degrees.

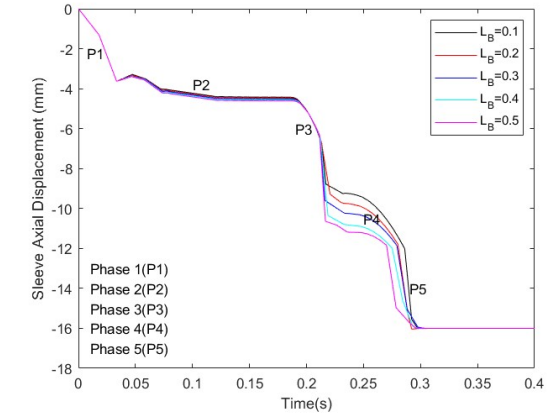

Figure 21: Variation of Lash Blocking Teeth in mm.

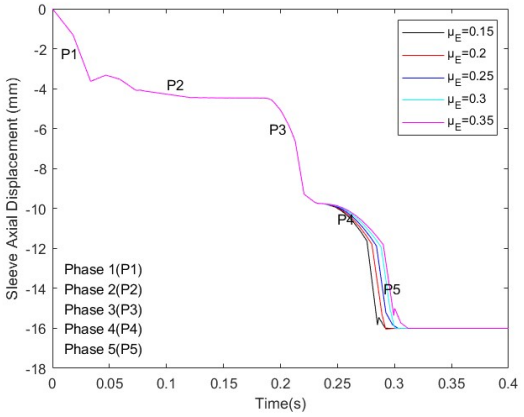

Figure 22: Variation of Engaging Teeth Friction Coefficient.

highest parameter value was 0.30 s, and for the lowest value 0.29 s.

In Figure 23, the results obtained by the model are illustrated for the variation of the tooth right angle of engaging teeth. The incremental change in the angle resulted in a minor adjustment to the required axial displacement for the synchronizer sleeve to initiate each phase affected. The parameter demonstrates influence on phases 4 and 5. There was a decrease in time with the increase in angle, where for the angle of 45^o, the time recorded was 0.29s, whereas for the angle of 65^o, the time measured was 0.27s. A similar behavior occurs when the parameter tooth left angle has been varied (Figure 24). The incremental change in the angle resulted in a minor adjustment to the required axial displacement for the synchronizer sleeve to initiate the phases 4 and 5. The displacement changes are greater, and therefore, generate a more significant variation in the final time. For this parameter, there was a decrease in time with the increment in angle, where for the angle of 25^o, the time recorded was 0.36 s, whereas for the angle of 40^o, the time measured was 0.28 s.

The last parameter evaluated for the engaging teeth was lash or free-play between teeth (Figure 25). Varying this parameter also changed the displacement of the synchronizer sleeve, affecting phases 4 and 5. Although it generated a change in the phases, especially in phase 5, the change in the final time was not significant. The parameter increment caused a small increase in the final time. The final synchronization time for the highest parameter value was 0.30 s, and for the lowest value 0.29 s.

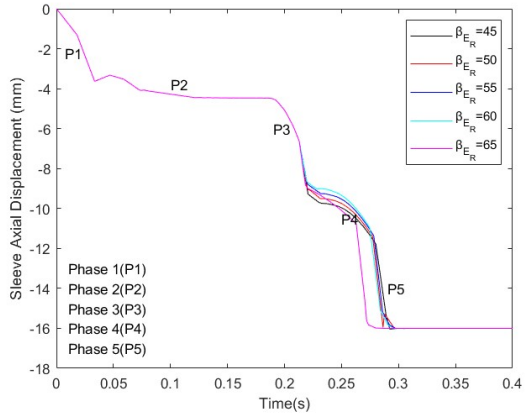

Figure 23: Variation of tooth right angle of Engaging Teeth in degrees.

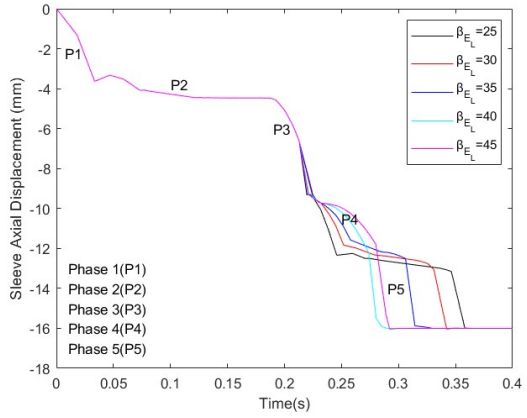

Figure 24: Variation of tooth left angle of Engaging Teeth in degrees.

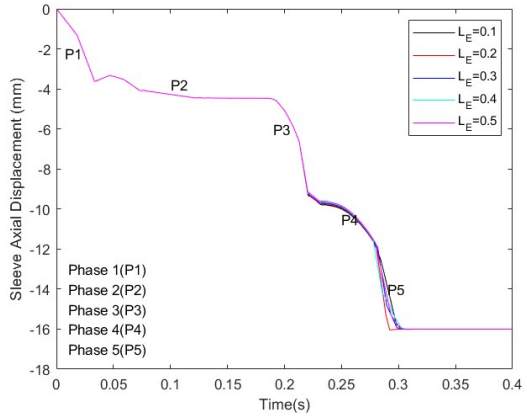

Figure 25: Variation of Lash Engaging Teeth in mm.

6 Conclusion

A gear shift mechanism is modeled in GT-Suite software. Structural and tribological design parameters of the mechanism are varied in order to analyze their real influence in relation to synchronization time. The first component analyzed was the detent. The analysis revealed that adjusting the groove angle of the detent had minimal impact on the ultimate synchronization time. The modification in the detent's friction coefficient yielded notably more pronounced effects on synchronization time, as the variations in friction resulted in a consequential increase in the overall synchronization time. The final parameter assessed for the detent was the groove height, and increasing its values showed an impact on reducing synchronization time.

The second component to be analyzed was the friction cone. The results obtained by model simulation indicate that increasing the cone angle causes an increasing in the synchronization time. The friction coefficient of the cone was also analyzed, where its increase produced a reduction in synchronization time. The increase in the maximum and minimum radius of the cone also showed to have their respective influence on the synchronization time, where the increase of both produced a reduction in time.

The last components to be analyzed was the blocking teeth (synchronizer ring) and engaging teeth (gear wheel). The first parameter evaluated for this component was the friction coefficient, which demonstrated results as expected. In both cases, the rise in the friction coefficient contributed to an increase in the final synchronization time, with this effect being more pronounced in the engaging teeth. The adjustment of the tooth right angle for both components revealed an impact on decreasing synchronization time as the angle increased, with this effect being more pronounced in the engaging teeth. The adjustment of the tooth left angle showed different behavior between the two components. Increasing the angle shows a tendency for an increase in time for the blocking teeth and a decrease in time for the engaging teeth. The last parameter evaluated was lash or free-play between teeth. The variation of this parameter had relatively minor effects on the blocking teeth while it exerted a subtle influence on increasing time, displaying a tendency as the parameter values increased for the engaging teeth.

The model created in GT-Suite demonstrated good performance in simulating the synchronization process, allowing for the evaluation of each phase of the process. The model enabled the analysis of the influence

of the studied parameters on the duration of each phase of the synchronization process. However, some factors that reduce synchronization time may have negative effect on NVH (Noise, vibration, and harshness). Especially the blocking teeth parameters, they are designed to slow the engagement and make it smoother. Therefore, any change in the parameters demonstrated here will have an influence on the synchronization time must be accompanied by experimental studies to evaluate their effect on vibration and noise in the synchronization system.

Future research could extend the present study by incorporating experimental validation of the simulated results, focusing on the NVH impacts of parameter changes to ensure that improvements in synchronization time do not compromise overall system performance. Additionally, the model could be expanded to include more complex gear-shifting scenarios, such as multi-stage synchronization or varying operating conditions, to evaluate the robustness of the proposed modifications under real-world applications. Investigating advanced materials and coatings for synchronization components could also offer insights into achieving better performance while maintaining durability and reducing wear. Finally, incorporating machine learning techniques to optimize parameter selection and predict synchronization behavior under diverse configurations could provide a more systematic approach to gear-shifting mechanism design.

Acknowledgements

The authors would like to acknowledge the support given by Centre of Vehicles for Sustainable Mobility of Faculty of Mechanical, Czech Technical University, Prague, Czech Republic.

Declaration of Conflicting Interests

The author(s) declare no potential conflicts of interest with respect to the research, authorship, and/or publication of this article.

References

BEDMAR, A. P. **Synchronization processes and synchronizer mechanisms in manual transmission: Modelling and simulation of synchronization processes**. Dissertação (Mestrado) — CHALMERS University of Technology, 2013.

HÄGGSTRÖM, D.; NORDLANDER, M. **Development of a Program for Calculating Gearbox Synchronization**. Dissertação (Mestrado) — Luleå University of Technology, 2011.

HOSHINO, H. Analysis on synchronization mechanism of transmission. In: **SAE Technical Paper Series**. [S.l.: s.n.], 1999.

HUANG, H.; GUHMANN, C. Model-based gear-shift optimization for an automated manual transmission. **Proceedings of the Institution of Mechanical Engineers, Part D: Journal of Automobile Engineering**, v. 289, p. 245–263, 2018.

HUANG, H.; NOWOISKY, S.; KNOBLICH, R.; GüHMANN, C. **Multi-domain modelling and simulation of an automated manual transmission system based on Modelica**. ***International Journal of Simulation and Process Modelling (IJSPM)***, v. 10, n. 3, 2015. Disponível em: <https://www.inderscience.com/offers.php?id=71377>.

IRFAN, M.; BERBYUK, V.; JOHANSSON, H. **Constrained Lagrangian Formulation for Modelling and Analysis of Transmission Synchronizer**. Göteborg, Sweden, 2015.

IRFAN, M.; BERBYUK, V.; JOHANSSON, H. **Modelling of Heavy Vehicle Transmission Synchronizer using Constrained Lagrangian Formalism**. In: ***International Conference on Engineering Vibration***. Ljubljana, Slovenia: [s.n.], 2015.

IRFAN, M.; BERBYUK, V.; JOHANSSON, H. **Failure modes and optimal performance of a generic synchronizer**. In: ***The 5th Joint International Conference on Multibody System Dynamics***. Lisboa, Portugal: [s.n.], 2018.

IRFAN, M.; BERBYUK, V.; JOHANSSON, H. D. Minimizing synchronization time of a gear shifting mechanism by optimizing its structural design parameters. **Proceedings of the Institution of Mechanical Engineers, Part D: Journal of Automobile Engineering**, 2019.

LI, J.; FENG, X.; JIANG, M.; ZHANG, Y.; WAN, L. **Modelling and simulation of synchronization and engagement for self-energizing synchronizer with multibody dynamics**. ***Advances in Mechanical Engineering***, v. 9, n. 3, 2017. Disponível em:

<https://journals.sagepub.com/doi/full/10.1177/1687814017691410>.

LIU, Y. C.; TSENG, C. H. Simulation and analysis of synchronisation and engagement on manual transmission gearbox. **International Journal of Vehicle Design**, v. 43, p. 200, 2007.

NEJAD, A. F.; CHIANDUSSI, G. Estimation of the synchronization time of a transmission system through multi-body dynamic analysis. **International Journal of Mechanical Engineering and Robotics Research**, v. 6, n. 3, p. 232–236, 2017.

QI, X.; YANG, Y.; WANG, X.; ZHU, Z. **Analysis and optimization of the gear-shifting process for automated manual transmissions in electric vehicles**. ***Proceedings of the Institution of Mechanical Engineers, Part D: Journal of Automobile Engineering***, v. 231, n. 13, p. 1751–1765, 2017. Disponível em: <https://journals.sagepub.com/doi/10.1177/0954407016685461>.

STOCKINGER, U.; SCHNEIDER, T.; PFLAUM, H. e. a. **Single vs. multi-cone synchronizers with carbon friction lining—a comparison of load limits and deterioration behavior**. ***Forsch Ingenieurwes***, v. 84, p. 245–253, 2020. Disponível em: <https://link.springer.com/article/10.1007/s10010-020-00406-1#citeas>.

SUN, S.; SHI, H. Design and optimization of automatic shifting mechanism for the tractor. In: **The 4th International Conference on Mechatronics and Mechanical Engineering (ICMME 2017)**. [S.l.: s.n.], 2017. v. 153.

VIJAY, K.; KUNAL, R.; MERUVA, K.; JATHAR, J. **C-Shaped Synchronizer Spring-theoretical Analysis and Validation**. [S.l.], 2012. Disponível em: <https://www.sae.org/publications/technical-papers/content/2012-01-2002/>.

ZAINURI, F.; SUMARSONO, D. A.; ADHITYA, M.; SIREGAR, R. **Design of synchromesh mechanism to optimization manual transmission's electric vehicle**. ***AIP Conference Proceedings***, v. 9, n. 3, 2017. Disponível em: <https://pubs.aip.org/aip/acp/article/1823/1/020031/584712/Design-of-synchromesh-mechanism-to-optimization>.

ZEMAN, T. **Model of gearbox gearshift with help of synchroniser clutch**. Dissertação (Master's thesis) — Czech Technical University, Prague, Czech Republic, 2019.